CHAPTER TWO

Advances and innovations in electrospinning technology

Pooya Davoodi[1,2,a] **Elisabeth L. Gill**[1,2] **Wenyu Wang**[1,2], **Yan Yan Shery Huang**[1,2]

[1]Department of Engineering, University of Cambridge, Cambridge, United Kingdom
[2]The Nanoscience Centre, University of Cambridge, Cambridge, United Kingdom

Abbreviations

2D Two-dimensional
3D Three-dimensional
AgNPs Silver nanoparticles
AM Additive manufacturing
CTS Critical translation speed
DC Direct current
FDM Fused deposition modeling
LEP Low-voltage electrospinning
MES Magnetic electrospinning
NFES Near-field electrospinning
PCL Polycaprolactone
PDLLA Poly-d,L-lactic acid
PDMS Polydimethylsiloxane
PEO Polyethylene glycol

2.1 Introduction

Fiber is a one-dimensional and high aspect ratio structure that widely exists in nature (i.e., spider silks and silkworm filaments) and has been extensively used in our daily life and industries, ranging from clothing fashion industry [1], wastewater treatment [2], to biomedical applications [3] and wearable electronics [4]. At a single thread level, individual fibers possess unique mechanical properties, including ultraflexibility, low bending resistance, and large surface-to-volume ratio; when processed into fiber mats or textiles, such large-scale fibrous structures could demonstrate bendability,

[a] Present address: School of Pharmacy and Bioengineering, Keele University, Keele, United Kingdom.

Biomedical Applications of Electrospinning and Electrospraying
ISBN: 978-0-12-822476-2
https://doi.org/10.1016/B978-0-12-822476-2.00004-2

stretchability, breathability, and high porosity, intriguing wide range applications in many areas. Numerous approaches have been developed to produce synthetic fibers with various materials, and among them, electrospinning is a broadly used and efficient method to produce micro-/nanoscaled fibers (fiber diameter ranges from 2 nm to several micrometers) [5]. Apart from electrospinning, most of other conventional fiber production approaches, such as wet and dry spinning, drag spinning, gel spinning, and three-dimensional (3D) printing, rely on the mechanical drawing or shear stresses alone to stretch and thin the fiber jet; thus, they usually struggle to produce ultrathin fibers with fiber diameter smaller than $\sim$10 μm without causing fiber breakage [6]. Electrospinning utilizes strong static electrical forces to pull and stretch the polymer solutions or melts into thin jets, leading to final micro-/nanofiber deposition. Such phenomenon was first being discovered and described over a century ago [7], but not until the early 1900s that the term "electrospinning" had been officially proposed [8]. Since then, the research and studies about this versatile and simple fiber production technique have been growing significantly [9].

With recent developments in materials science and nanotechnology, new materials have been incorporated with the electrospinning technique, such as conducting materials, energy generating materials, and biocompatible and bioactive materials. Electrospun micro-/nanoscaled fibers that are functionalized with these new materials have not only retained the physical merits of ultrathin fibers, such as high aspect ratio, flexibility, directionality, and high porosity, but also opened up novel fibrous and textile device configurations and applications. For example, the use of piezoelectric polymers has enabled a range of inherently flexible and transparent energy harvesters and self-powered sensors [10,11]. Composite material fibers made with polymers and metals or ceramics have shown promising application potentials in novel sensing and optoelectronic devices [12,13]. At the same time, these emerging applications demand more precise, convenient, and customized control of the morphologies and patterns of the electrospun fibers. Therefore, efforts have been invested to modify and adapt the electrospinning setups and working conditions, and to combine fiber spinning with other advanced processing techniques (i.e., 3D printing and microfluidics).

In this chapter, we aim to provide a comprehensive description of the recent innovations and technical advances of electrospinning. In order to readers who are not familiar with electrospinning to effectively read this chapter, a brief introduction of the physical principles and basic setup designs of electrospinning is provided at the beginning, followed by discussions of

major and universal experimental factors that could affect the fiber spinnability in the technique, including polymer solution properties, ambient, and operation parameters. Next, we focus on the recent application-driven advances and innovations in electrospinning technique. Various approaches to modify the conventional electrospinning setups to acquire controlled and designed fiber patterns will be discussed first, including modifying nozzle and collecting substrate, controlling and directing fiber deposition, and stabilizing fiber jet, followed by introducing novel electrospinning techniques that are combined with other polymer processing technologies, such as additive manufacturing (AM) and microfluidic devices.

2.2 Electrospinning: the underpinning physical principles

Electrospinning is similar to other spinning techniques in that a tensile force draws a fiber from a spinnable source; however, it differs in the manner of fiber initiation [14]. The majority of other spinning techniques utilize mechanical initiation in the form of spindles or mechanical dragging, whereas in electrospinning, this effect is substituted with Coulomb's force from the application of a strong electric field. Briefly, a viscous polymer solution or melt is fed through to a syringe needle at low flow rate until a droplet of solution collects at the tip. As shown in Fig. 2.1, a high electrical charge is

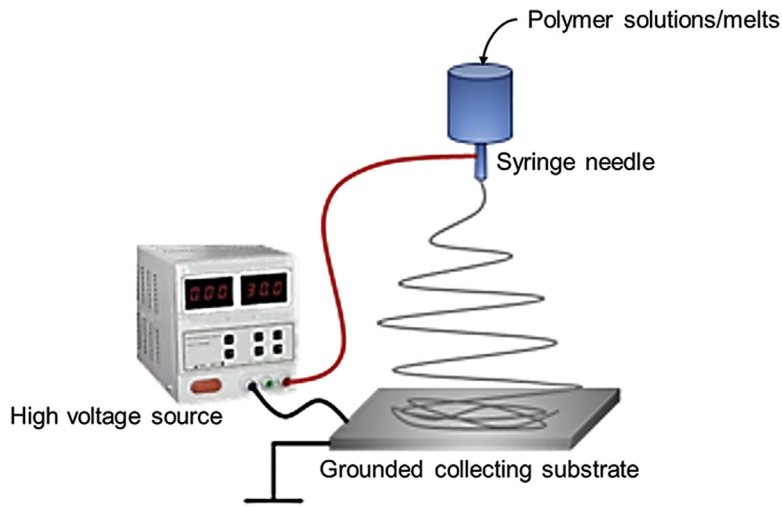

Figure 2.1 Schematic showing the basic setup configuration of electrospinning.

applied to the solution or melt either within the syringe or at the syringe needle, which is directed toward an oppositely charged collecting substrate. This exposes the droplet on the tip of the syringe to an electric field, exerting a tensile force in the same direction as the solution's internal electrostatic self-repulsion. A "Taylor cone" or deformation appears in the droplet just beyond the point where the resistive forces of droplet surface tension and solution/melt viscosity counterbalance the tensile force [6]. This formation initiates the ejection of a fine polymer jet from the apex of the cone toward the collecting substrate [15]. During the movement of the jet between the nozzle and the collecting substrate, the solvent vaporizes and a solid polymer fiber is collected. When the collecting substrate is greater than a few millimeters away, the self-repulsion of the polymer jet, due to Coulomb's force, gravity, and aerodynamic effects, causes chaotic bending instability [16,17]. This results in the polymer jet adopting a spinning motion that elongates the jet and consequently the collected fibers thin to a micro- to nanoscale, which concentrates the charge density within the fiber. Due to that bending instability [18,19], the deposition of fibers produced by conventional electrospinning creates random fiber packing.

Through careful optimization of the process instrumentation and working parameters of far-field electrospinning techniques, polymer fibers have been fabricated with diameters ranging between ~ 3 nm and a few micrometers [20]. Given the complexity of the process and high number of processing parameters, there is great scope for innovation with subtle variations extending product versatility. As one example, some have exploited the effect of the polymer jet splitting during transit to create such ultrafine fibers [21]. The section below thematically describes the influence of the key parameters and how these can be manipulated to create various fiber morphologies and fibrous designs.

2.3 Properties influencing spinnability of polymer solutions

Electrospinning setups typically include several basic parts: a high-voltage power supplier (usually a direct current power source), a conductive nozzle, a syringe pump used to control solution flow rate, and a grounded substrate for collecting fiber products [22]. During electrospinning, many factors can influence a jet movement and consequently the properties of final products. These factors include the following[22,23]: (a) solution properties (molecular weight, polymer molecule architecture, polymer

concentration, solvent, conductivity, surface tension, and viscosity), (b) ambient parameters (temperature, relative humidity, airflow and pressure around the setup, and ambient gas), and (c) operating parameters (applied voltage, solution flow rate, nozzle material and geometry, substrate material and geometry, and the distance between a nozzle and substrate). Properties of the polymer solution should be the first consideration when determining the applied voltage and other experimental conditions for a desired fiber continuity and morphology.

2.3.1 Solution properties

Surface tension acts to minimize the energy at the air—solution interface through lowering the surface area and forming droplets [16], whereas viscosity acts as a resistive force to sudden changes in solution jet shape and maintains a smooth surface [24,25]. In the case of spun fibers, they oppose one another. At low polymer concentration, surface tension can overpower viscosity, causing a beaded fiber, bead-on-string, or nanoparticle morphology [26,27]. The reverse happens as polymer concentration, and therefore molecular entanglement increases. Viscous effects dominate and this favors the fabrication of smooth and defect-free fibers [28]. Hence, adequate polymer concentration is a prerequisite to attain fibers at all [29,30], as at a molecular level, there is a threshold concentration for entanglement [31,32]. Examples of the transition from bead-on-string morphology to smooth uniform fibers with increasing polymer concentration have been demonstrated, as exemplified in Fig. 2.2a—c [25,36,37]. This is also dependent on the molecular weight of the polymer as longer chain molecules favor entanglement more than short-chain alternatives. Fiber diameter also generally increases with increasing viscosity as this increases the resistance of the polymer jet to deformation by elongation [27]. Another critical balance of forces takes place on the ejected polymer jet as evaporation of the solvent takes place and it forms a fiber. Surface tension acts on the polymer jet to maintain a circular cross section, while the tensile force provided by the electric field stretches it. Sufficient polymer concentration is also required to prevent capillary breakage and Rayleigh instability [28], otherwise this also leads to beaded fibers.

The volatility of the chosen solvent affects the rate at which the fibers will solidify in the spinning process. Solvents with high volatility ensure that the fibers are dry upon reaching their collecting substrate and attain a circular cross section. Alternatively, in some situations, it can be desirable

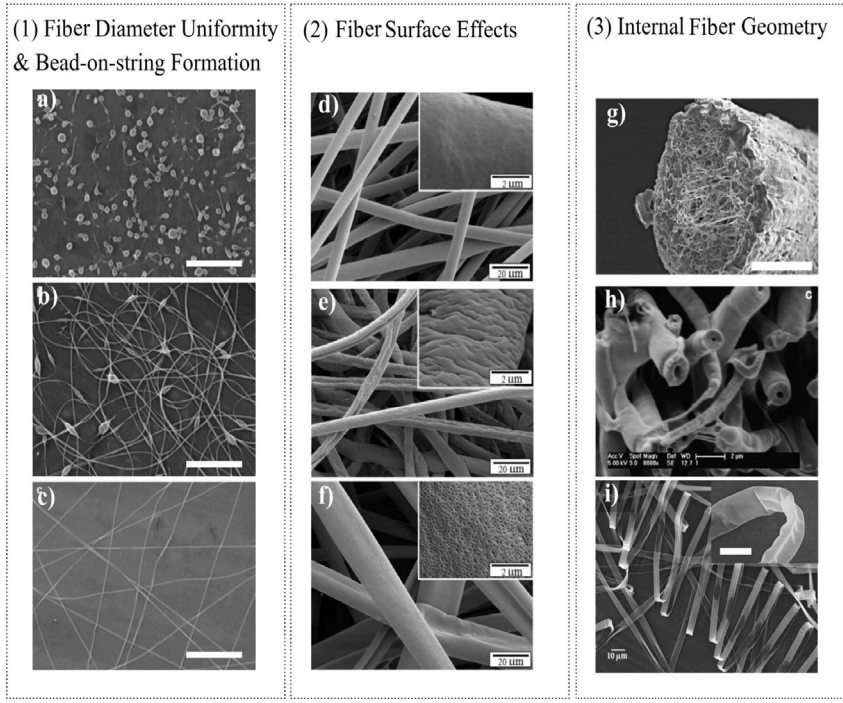

Figure 2.2 Control of electrospun fiber morphology. Polymer concentration and solution viscosity can lead to (a) electrosprayed beads, (b) bead-on-string, or (c) smooth fiber production [25]. Scales represent 5 μm. Solvent and atmospheric conditions can yield (d) smooth, (e) rough, and (f) nanoporous fiber surface morphologies [33]. Solvent conditions, nozzle configuration, and solution properties can be used to design internal fiber geometry, alternative to solid fibers, including (g) internal nanoporosity [34] (link: https://pubs.acs.org/doi/10.1021/acsami.8b17955), (h) hollow fibers [35], and (i) polymer ribbons [21]. Scales in (g) represent 1 μm, (h) 2 μm, and (i) 10 μm.

to have fibers spun wet, dry out gradually, and even merge with their neighbors to form mechanically strong interconnected fiber junctions [38]. At the other extreme, utilizing highly volatile solvents can design surface porosity and other surface textures on individual spun fibers through inducing phase separation during the process of fiber solidification. These nanoscale surface effects increase the fiber surface-to-volume ratio, a quality that is of interest for filtration and drug delivery applications for its efficacy in trapping small particles within nanopores (Fig. 2.2d–f) [33,39,40]. Manipulation of solvent properties can also extend to inducing porosity in fibers internally as was recently studied in, e.g., Fig. 2.2g [34].

Overall solution conductivity affects the surface free charge at the fiber surface, determining the charge density along the polymer jet [41]. It is essential to facilitate the electrostatic tensile force on the solution droplet and ensuing polymer jet to be characteristic of electrospinning. Increasing the solution conductivity is a direct way to increase the electrostatic tensile drawing force exerted on the polymer jet. This makes a solution more readily electrospun and increases the elongation effect on the polymer jet, which can be another strategy to decrease fiber diameter [42,43] and create a smooth fiber surface through maximizing the surface area [25]. Consequently, this also inherently increases the bending instability and disorder in the deposited fibers. This strategy has been explored by several groups through the addition of salt [44], such as NaCl [45], to enhance solution conductivity of PDLLA (poly-d,L-lactic acid) and other polymers. This demonstrated improved solution electrospinning behavior and yielded thinner fibers; furthermore, the addition of salt created surface roughness on the spun fibers.

2.3.2 Ambient parameters

The environmental factors that influence electrospinning processes can be logistically more challenging to control but undoubtedly have a considerable impact on spun fiber morphology [46–49]. These include surrounding temperature, humidity, and air velocity. Principally, this affects the rate of solvent evaporation. An increase in surrounding temperature has a complex overall effect: it increases the rate of evaporation, which can produce a rougher fiber surface. Localized heating of the polymer solution can also increase solution concentration and viscosity [47], and in some cases, this can be exploited to create thinner fibers [49]. Local airflow within a chemical safety hood is another indirect means to accelerate the rate of solvent evaporation, which like surrounding temperature may affect the fiber surface for some polymer solutions and be utilized to induce phase separation. Humidity can have varying effects on fiber topography through vapor-induced phase separation as shown by Moroni and et al. [46]. In the case of certain inorganic solutions that are immiscible in water, it can cause phase separation to the point at which the solution can no longer be spun [29]. Humidity can drastically change the solidification processes of polystyrene, for instance, and this can be exploited by smooth, porous,

or wrinkled fibers [29,33,50]. Unlike ambient temperature and flow rate, which affect electrospinning processes more universally, the influence of humidity is more specific to the solution conditions.

2.3.3 Operating parameters

The operating conditions that affect electrospinning processes include the following: solution flow rate, nozzle tip size and geometry, the applied voltage, the electric field that creates with a distanced substrate, and the substrate conditions. Without an adequate polymer flow rate, electrospinning processes cannot be maintained. At excess, high flow rate will produce much thicker or even beaded fibers [51], partially due to the rate of solvent evaporation being reduced and a greater influence of surface tension. One study constructively used the effect of fiber beading through optimizing polycaprolactone (PCL) concentration, the applied voltage, and working distance to produce "self-assembled" honeycomb patterns [36]. In addition to voltage and working distance, nozzle conditions can also affect solution flow rate. The size of the electrospinning nozzle directly influences the size of the initial polymer jet and the nozzle conductivity also has some influence over the overall solution conductivity. If the solution receives electric charge from inside the syringe, a conductive nozzle might encourage charge dissipation before spinning takes place, whereas if charge is imparted at the nozzle, the nozzle conductivity is the sole component which determines efficient charge transfer. Various works have innovated nozzle design to create core–shell and hollow fiber morphologies with the use of sacrificial materials [35] (Fig. 2.2h).

The application of voltage to polymer solution is the key distinguishing feature of electrospinning from any other fiber spinning techniques. By definition, potential difference between the source and the collecting substrate provides the threshold tensile force required to initiate fiber formation. The electrostatic forces that a droplet of polymer solution experiences during the intrinsic Taylor cone formation of electrospinning are twofold: the tensile Coulomb force in the direction of the collection substrate and the repulsive force due to surface charge accumulation. Once a polymer jet is initiated, the electrostatic forces stretch the jet up until the point of complete solvent evaporation or when the fiber is collected. Aside from the aforementioned solution properties, the magnitude of the electrostatic force is a function of the electric field strength. Both the applied voltage and the working distance between the suspended droplet and collecting substrate determine that

magnitude. Increasing the applied voltage has a clear effect on the spun fiber diameter [52]; however, this relationship is complex and subject to the other parameters. One can argue that increasing the applied voltage directly increases the tensile force on the polymer jet, so the stretching effect would be greater. Alternatively, a high voltage might accelerate the jet toward the collector so that the fiber is in transit for less time and accordingly is less stretched [53]. Another explanation could be that high voltages enhance the flow rate of a solution leading to thicker fibers, as the strength is simply pulling more material through the syringe. To support that, there is a clear correlation that at excess applied voltage, beaded fibers begin forming and there is an increase in "whipping" behavior of the polymer jet [43,51].

Altering the working distance is another direct means to manipulate the electric field and influence fiber diameter. As the working distance between the Taylor cone apex and collecting substrate increases, the electric field intensity decays in a rapid and nonlinear way [54]. It also largely determines the time that the polymer jet remains in transit, which effects the extent of the bending instability and evaporation rate of the solvent. Traditionally, electrospinning processes utilize a working distance between 10 and 20 cm to permit thorough solvent evaporation and collection of dry fibers. To create a sufficient electric field for fiber initiation, the applied voltage often is in a range of 10−40 kV, and the consequent bending instability generates fibers in a random network. When the applied voltage is high and the working distance is comparatively short, this generates a very intense electric field and can induce electric arcing, highlighting the importance of selecting experimental parameters within an optimal threshold.

2.4 Advances and innovations in electrospinning for application-driven research

The factors mentioned in the previous sections may play different roles in different electrospinning systems. Thus, depending on ultimate applications anticipated for a product, the process parameters can be precisely adjusted by an operator to control the properties of the final products. Further, to impose a more precise control on final products morphology, geometries, and arrangement, the electrospinning processes have been modified through the following:

(a) Redesigning and improving the traditional setups based on a particular application (e.g., modifying nozzle and collecting substrate, controlling and directing fiber deposition, and stabilizing jet).

(b) Transition from far-field electrospinning to high-resolution near-field electrospinning (NFES) of controlled fiber deposition.
(c) Transition from the use of high voltage to low voltage for continuous electrospinning fiber patterning.
(d) Transition from electrospinning to high-resolution electrowriting.
(e) Combining electrospinning with other polymer processing technologies such as AM and microfluidic devices.

2.4.1 Redesigning the traditional electrospinning

As shown in Fig. 2.3, the improvement of traditional electrospinning has been mainly focused on dispensing nozzles and collecting substrates. Therefore, in addition to a traditional single nozzle [55–57], coaxial [58,59] and triaxial nozzles [60,61], multinozzle [62,63], and side-by-side/multichannel nozzles [64] have been successfully introduced for the fabrication of core/shell, triaxial, multichannel, Janus, beaded [25], bead-on-string [65], necklacelike [66], colloidal [67], bamboolike [68], and ribbon fibers [21]. Along with these modifications, needleless electrospinning via rotating disk [69] and bubble formation [70] techniques have been also introduced to achieve nanofibrous structures. The proposed modifications on collecting substrates include various rotating collectors (e.g., rotating drums and disks, wire drums) [71], water bath [72], and a dynamic liquid substrate for collecting nanofiber yarns [73]. (These modifications were thoroughly reviewed elsewhere [6]).

Alternatively, the sensitivity of the electrospinning jet to local substrate electric field profile can be advantageously used to guide fiber deposition in 2D and even 3D. These methods focus on the final stages of the fiber-drawing process, pulling the traveling jet away from the region of bending instability, and directing it to a specific target electrostatically [74]. For instance, collection electrodes and collection substrates with ridges and micropillars, parallel electrodes [75], dual collecting rings [76], adding nanomaterials triggered and guided by auxiliary fields (e.g., magnetic field) to the polymer solution, and patterned conductive substrates [77] or sharp edges or pins electrodes to ground an incoming jet [74,78–80] have been successfully utilized to create aligned fibers [81,82].

As the formation of free-standing fibrous structures has found many applications in biomedical fields, the two simple fabrication methods of such structures are presented in details. The simplest approach for the deposition of aligned fibers on a substrate or over a narrow gap was proposed by

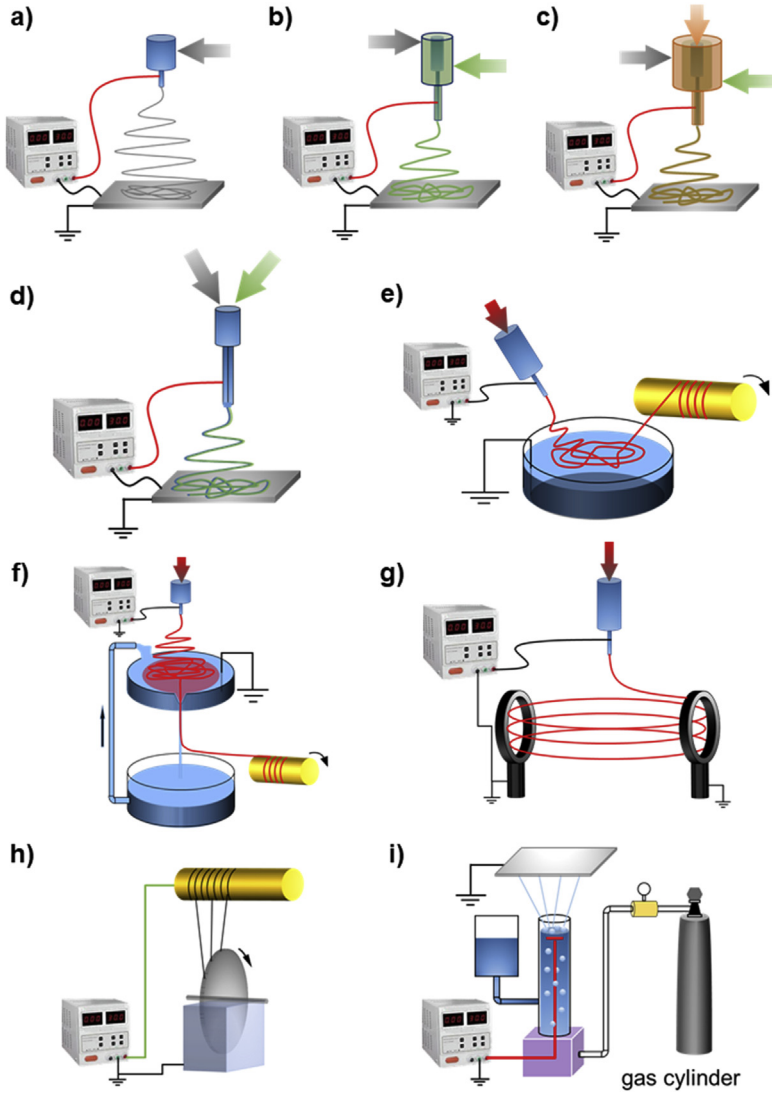

Figure 2.3 Schematic illustrations of various electrospinning setups reported in the literature: (a) traditional electrospinning setup, (b) coaxial electrospinning, (c) triaxial electrospinning, (d) multichannel electrospinning, (e) electrospinning via fiber collecting water bath, (f) a dynamic liquid substrate for collecting nanofiber yarns, (g) collecting aligned nanofiber using dual collections rings, (h) needleless disk electrospinning, and (i) needleless bubble electrospinning. *All schemes were redrawn with modifications.*

Xia et al. [83]. They changed the geometry of a grounded substrate from a flat surface into two conductors separated by a void gap (Fig. 2.4). Such a collector could be simply manufactured by placing two strips of electrical conductors such as highly doped silicon and metal bars together or by using two pieces of aluminum foil, where the gap could change up to several centimeters depending on the desired applications. In contrast to conventional electrospinning, in this configuration, the electric field lines are split into two fractions pointing toward the conductors at each side of the gap. This electrical field deviation imposes two sets of electric forces onto nanofibers and consequently aligns them uniaxially across the gap, where their longitudinal axes oriented perpendicular to collector edges. The stacking density of fibers deposited over a gap is proportional to the collection time and inversely depends on the gap width. The longer collection time and the narrower gap yield denser arrays. However, their results demonstrated

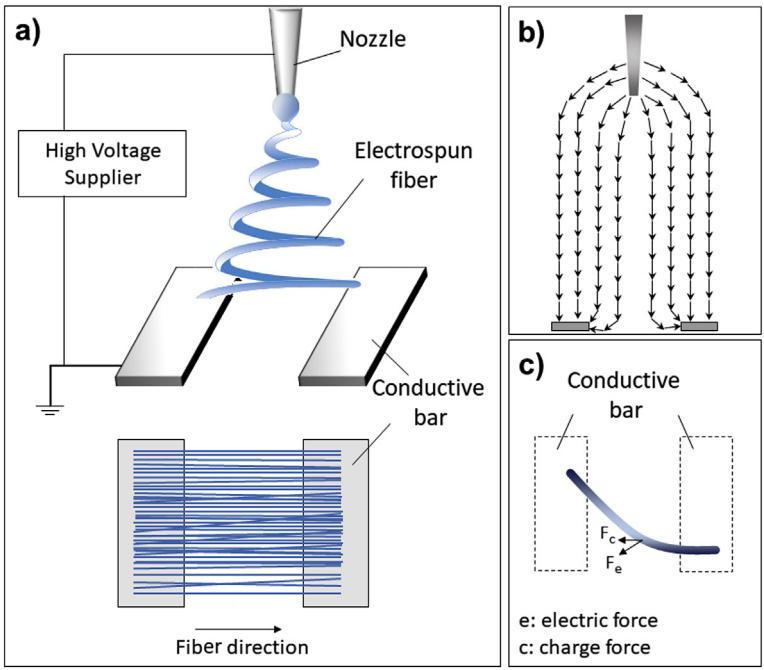

Figure 2.4 Schematic illustrations of the setup for electrospinning for generating uniaxially aligned nanofibers. (a) Modified setup configuration with the parallel conductive bars as collecting substrates. (b) Schematic illustration showing the distribution of static fields. (c) Schematic illustration showing the electric and charged forces exerting on the fiber jet.

that thinner fibers (diameter <150 nm) are quite unstable across a gap >1 cm, as the fibers cannot tolerate their own weight and electrostatic repulsion forces applied by other fibers. To deposit fibers across a wide gap beyond several micrometers, it was suggested to use a temporary and nongrounded substrate for supporting fibers. In addition to uniaxially aligning fibers, it would be also easy to fabricate a multilayer nanofiber structure by controlling the configuration of electrodes [9].

Another approach proposed for patterning aligned fibers is to directly manipulate the electrospinning process through incorporating stimuli-responsive materials such as magnetic nanoparticles to the solution and directing fiber orientation via applying an external stimulus (e.g., magnetic field) [84]. Therefore, magnetic electrospinning was reported as a facile and effective technique that could simply fabricate highly aligned fibers and multilayer lattices over a large area. The fiber meshes could also be easily transferred to other substrates or over microfluidic channels for more sophisticated applications. In this method, a small amount (>0.5 wt%) of magnetic nanoparticles was mixed with a polymer solution to magnetize it, and the solution is electrospun in the presence of a permanent magnetic field imposed by a pair of parallel-positioned permanent magnets. While both magnetic and electric fields can attract fibers to a collecting substrate, the magnetic field plays an essential role in aligning them over the gap between the two magnets (Fig. 2.5) [85,86].

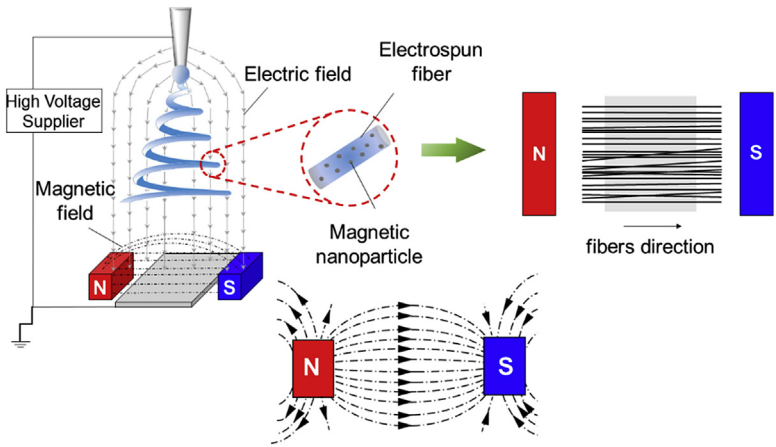

Figure 2.5 Schematic illustration of the setup used in the magnetic field–assisted electrospinning technique for fabricating aligned nanofibers.

Furthermore, to fabricate an electrospun fiber structure over a void gap with a curved geometry, researchers substituted solid collecting substrates with sacrificial conductive materials or an electrolyte [87]. The fluidic nature of the electrolyte provides flexibility in shaping the grounded collector and patterning according to the shape of a narrow channel. The ease of removing electrolytes after depositing fibers allows formation of a free-standing structure without conducting further mechanical or chemical peel-off processes for transferring fibers over the channel.

2.4.2 Transition from far-field to near-field electrospinning

High-resolution images of an electrospinning show that a polymer jet is made of three characteristic regions: a Taylor cone, proceeded by a stable straight region of around 10–30 mm, known as near-field region, before a bending instability takes effect [88] (Fig. 2.6).

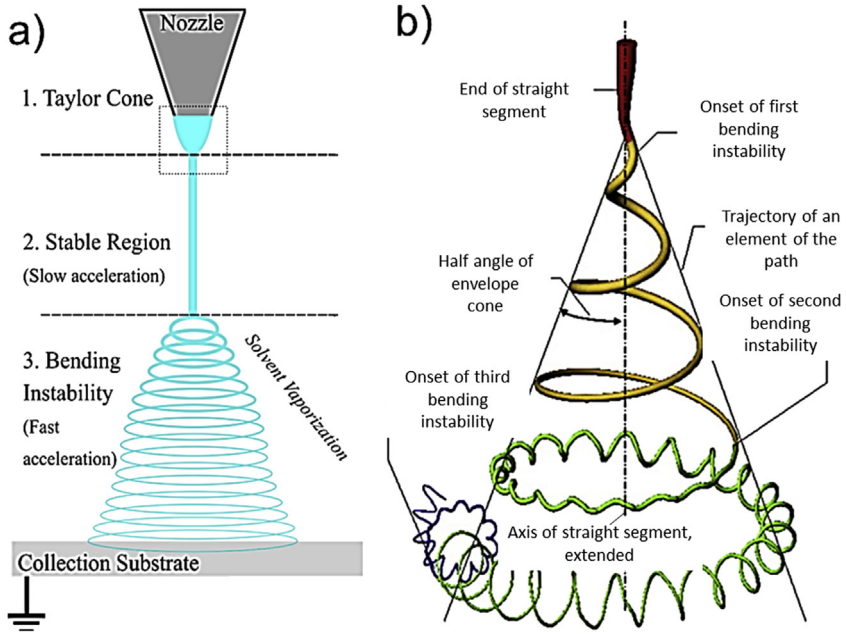

Figure 2.6 The region of bending instability characteristic of electrospinning techniques. (a) The point at which the bending instability establishes and its relation to jet stabilization strategies, (b) Solution jet path of traditional electrospinning. *Adapted from Reference Reneker, D.H., Yarin, A.L. (2008). Electrospinning jets and polymer nanofibers. Polymer 49(10), 2387–2425 under CC BY-NC-ND 3.0 license.*

In fact, the viscoelastic properties of the polymer jet should be able to overcome the Rayleigh instability which may break the jet into droplets [89,90], that is observed in electrospraying process [91–93]. As the polymer stream moves through the stable region, it creates a conductive path for the electric current to pass through. The velocity of the jet within this region was estimated to be ~1–15 m/s [94,95]. Therefore, the estimated critical length of the stable and straight jet can be calculated via Eq. (2.1):

$$L = \frac{4kQ^3}{\pi\rho^2 I^2}\left(\frac{1}{R_0^2} - \frac{1}{r_0^2}\right) \tag{2.1}$$

where $R_0 = (2\sigma Q/\pi k\rho E)^{1/3}$, σ is the surface tension, Q is the polymer solution flow rate, k is the electrical conductivity of the solution, ρ is the solution density, E is the electrical field strength, I is the current passing through the jet, and r_0 is the jet initial radius [96,97].

Based on the above information, the key to patterning electrospun fibers with greater precision is to dampen the influence of the chaotic jet bending instability on fibers. This can be achieved through redesigning the process around the stable region on the jet and preventing the bending instability from establishing in the first place. This is the central premise behind NFES [98], which reduces the distance between the Taylor cone and a collecting substrate to a millimeter scale as well as reducing the applied potential difference at the source by an order of magnitude. Thus, the overall electric field strength required for electrostatically driven fiber initiation is maintained. Adjusting these parameters enables direct writing of straight, coiled, or helical polymer fibers through matching the feed rate of solution with the translation speed of either the deposition substrate or the electrospinning spinneret itself. The ability to design the path of the translating component of NFES configurations allows drawing of complex 2D patterns in a versatile manner akin to 3D printing [99–101].

Omitting the region of bending instability does reduce the elongation effect on the polymer jet; thus, the fibers produced tend to be larger. Additionally, as the jet has a shorter travel distance, the solvent has less opportunity to evaporate and the fibers may still be wet immediately after patterning unless the solvent is volatile. In some cases, the wet fibers may adopt a semicircular cross section [102], as opposed to a rounded fiber or merge with neighboring fibers [38,103]. Another factor to consider is that the deposited fibers may retain some residual charge, which can act against achieving dense

fiber alignment through repelling the incoming jet [104]. Use of coagulation baths as a collecting substrate is one strategy to avoid this issue while ensuring thorough removal of solvents [105].

2.4.3 Transition from high-voltage to low-voltage electrospinning

Another research direction developed using NFES to pattern fibers in 3D is to reduce the applied voltage further through initiating jet formation with high voltage to begin with before significantly lowering it [101] or the use of physical objects or "initiators" to draw out the polymer jet [99,106]. Here, both stabilized jet and substrate modification control and direct a patterning process. Bisht et al. developed a highly elastic polymer ink that can draw dry fibers spanning between micropatterned posts at voltages as low as 200V [99]. Recently, Huang et al. proposed a new technique in which a motorized XYZ-stage was integrated with NFES to fabricate and precisely position fibers over a gap of several millimeters [107–109]. To achieve this goal, they employed an initiator that facilitated the formation of the polymer jet under an applied voltage. Subsequently, fibers were drawn between the two initiators due to moving the nozzle between these initiators. A drawback of the proposed technique is the solvent evaporation from a predeposited solution that confines its application for patterning only across narrow gaps to lessen the adverse effect of solution drying [107–110].

Recent development in near-field techniques has further lowered the operating voltage to the range of 100V [108]. Low-voltage electrospinning patterning introduced by Huang's group utilizes both mechanical and electrical forces for fiber initiation process, in addition to the mechanical stretching of the fiber against a collection substrate (Fig. 2.7). The presence of the initiator can promote the onset of fiber jetting and enhance the fiber stretching and thinning process. When the initiator is close to the nozzle position, even at a voltage of around 100 V, the focusing of the electric field can locally reach $\sim$2500 V/cm. As the substrate moves toward the center of the substrate, the electric field distribution becomes more symmetrical which allows fibers to be accurately deposited at a predetermined position. Lowering the applied voltage in electrostatic processing can minimize potential damages on bioactive components, provide greater flexibility and higher safety when combined with 3D printing mechanisms.

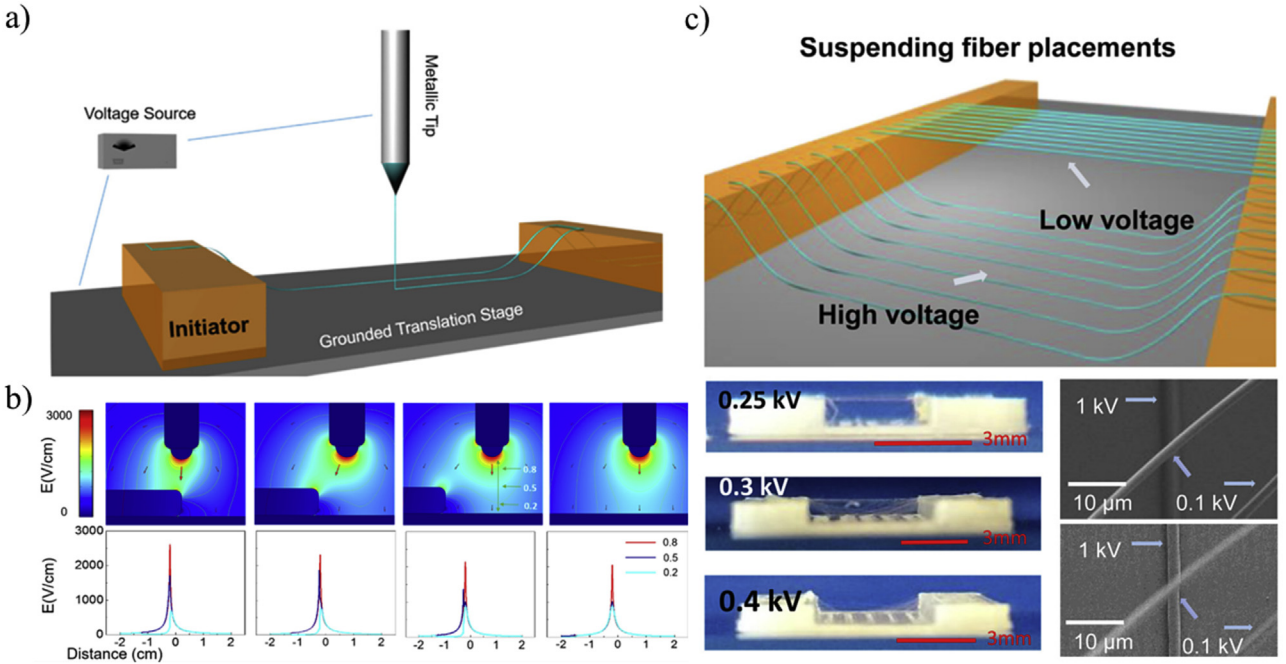

Figure 2.7 (a) Schematic illustration of figure low-voltage electrospinning setup; (b) Simulation of the electric field distribution with the moving of the initiator relative to the nozzle; (c) Schematic illustration of fiber deposition by adjusting the voltage application over a gap; (d) Fibrils bridging over a gap of 2 mm deep with a separation distance of 2.4−3.2 mm. Fibers were created using voltages of 0.25, 0.3, and 0.4 kV, respectively. SEM images show the effect of voltage on fiber deposition on the substrate (at 1 kV) and suspension (at 0.1 kV) over the gap. *Adapted from Reference Li, X., Li, Z., Wang, L., Ma, G., Meng, F., Pritchard, R.H., Gill, E.L., Liu, Y., Huang, Y.Y.S. (2016). Low-voltage continuous electrospinning patterning. ACS Appl. Mater. Interfaces 8(47), 32120−32131 under Creative Commons Attribution 4.0 International license-Open access.*

2.4.4 Transition from electrospinning to electrowriting

Scanning tip electrospinning, high-precision deposition electrospinning, and NFES are different direct writing solution electrospinning, in which an automated XYZ-stage is used as a collecting substrate [111]. The short collection distances between nozzles and substrates, together with moving stages presented in these techniques, yield a high relevance of fiber deposition in a predetermined fashion. However, the production rate in such techniques is extremely low of the order of 0.7 μg polymer per hour [112]. Researchers also reported electrospinning a PCL/dimethyl formamide/methylene chloride solution into a polyethylene glycol (5 wt%) aqueous bath placed on an automated moving stage [113]. This technique produced fibrous structures with 205 ± 61 μm fiber diameter and rough surface morphology, compared to structures produced with fused deposition modeling (FDM). Lee et al. also demonstrated a new approach in which a cylindrical side electrode and a thin, sharp, and moving collector controlled fiber deposition [114]. Scaffolds produced via their method benefited from uniform fibers with submicron diameter and constant morphology.

Compared to solution electrospinning, melt electrospinning can produce fibers of several micrometers in diameter. Moreover, electrified jet in molten electrospinning does not exhibit dynamic motions observed in conventional electrospinning and reduces charge accumulation on deposited fibers, enabling more accurate stacking fibers. These advantages can be attributed to the lack of charge solvent and the higher viscosity of the fluid. In addition, the lack of chaotic motions in melt electrospinning significantly reduces complexities required for designing XYZ-stages, where straight fibers can be drawn for speeds ranging from $\sim$8 to 20 mm/s compared to speeds ($\sim$50−150 mm/s) required in NFES [115]. Although melt electrospinning writing is the most similar technique to FDM, there are some important distinctions between these two methods including much smaller fiber diameter, lower pressure at the spinneret tip, and much larger distance between the nozzle and collector in melt electrospinning (Fig. 2.8).

The formation of a stable jet is a prerequisite for a controlled deposition of electrospun fibers on a stationary substrate. However, in the case of a moving platform, the formation and deposition of continuous and unbeaded fibers in a predictable and repeatable manner requires further adjustments and controls over key processing parameters including polymer flow rate in the nozzle, collector speed, electric field, while the viscosity and charge of the fluid define the properties of the molten polymer [117]. Polymer

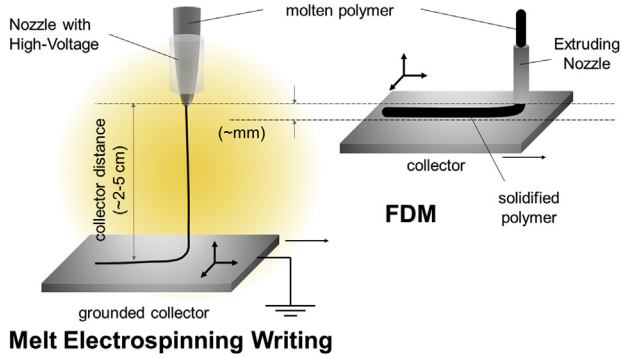

Figure 2.8 The distinctions between fused deposition modeling (FDM) and melt electrospinning writing. *Redrawn from Reference Dalton, P.D., Vaquette, C., Farrugia, B.L., Dargaville, T.R., Brown, T.D., Hutmacher, D.W. (2013). Electrospinning and additive manufacturing: converging technologies. Biomaterials Science 1(2), 171–185.*

melts with high viscosity and low conductivity are suitable for melt electrospinning writing applications to create 3D structures through controlled fiber patterning. Thus, all the parameters should be precisely and simultaneously tuned in order to fabricate highly ordered structures in laboratory scales and even in large scales.

For melt electrospinning writing (Fig. 2.9a), when polymer mass flows from the spinneret to the jet and then onto the collector are not adjusted, it may cause inconsistency and undesired sectional oscillation (known as "pulsing") of the fiber diameter or bead formation. Pulsing can affect the fiber deposition particularly when the moving stage changes the direction. In addition to the flow rate [120], accelerating voltage can cause pulsing effects and introduce artifacts into the printed construct due to the oscillation of jet flow rate. When the applied voltage is slightly lower than the optimized voltage at a fixed collector distance, the pulsing occurs as the forces which lead to jet stretching are not constant. This condition is even worse when the voltage is considerably lower and leads to the formation of long beads on fibers (Fig. 2.9b). Overall, to avoid these undesired process instabilities, the operator should limit the mass flow injected through the spinneret or stabilize the mass flow of the polymer jet via increasing the applied voltage which increases the electrical field strength [118].

To successfully deposit fibers on a moving substrate, the moving speed (S_c) should be higher than the ultimate jet speed (S_j), known as the critical translation speed, CTS. For a melt electrospinning writing setup operating well beyond CTS, the fiber can be stretched to obtain a submicron diameter size. On the other hand, for a transition speed below CTS, a jet buckling

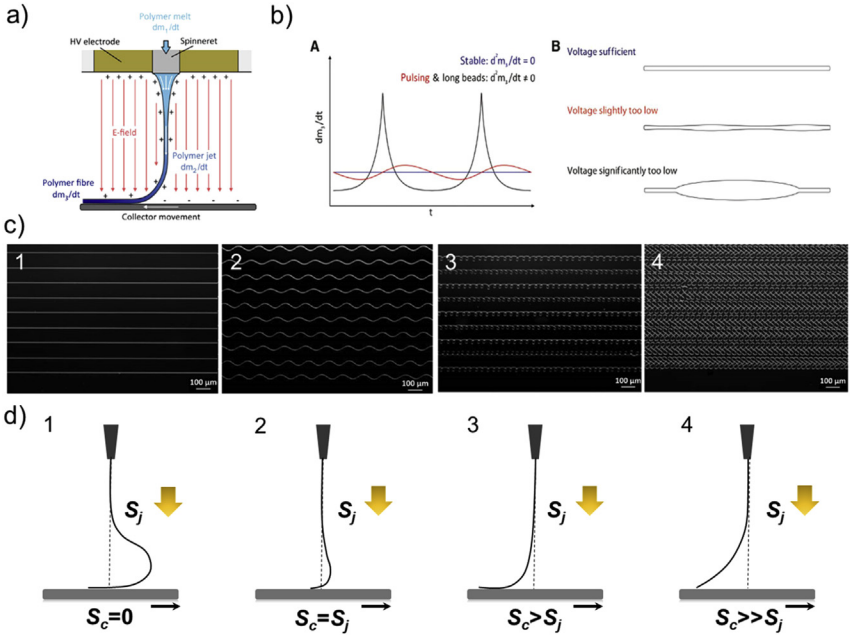

Figure 2.9 (a) The schematic illustration of melt electrospinning writing; (b) the effects of flow rate and voltage on the fiber geometry: (A) Mass flow rate deposited on the moving substrate (dm_3/dt) versus time. The dm_3/dt is proportional to the polymer flow rate of the jet. (B) The morphology of fibers collected on the moving substrate; (c) jet buckling and nonlinear patterns on the substrate. (d) Different scenarios for the relationship between jet speed (S_J) and collector speed (S_C). *Reproduced from Reference Gernot, H., Almoatazbellah, Y., Andrei, H., Jodie, N.H., Tomasz, J., Jürgen, G., Paul, D.D. (2016). Fibre pulsing during melt electrospinning writing. BioNanoMaterials 17(3–4), 159–171 under the Creative Commons CC BY-NC-ND 3.0 license; Redrawn from Reference Brown, T.D., Dalton, P.D., Hutmacher, D.W. (2011). Direct writing by way of melt electrospinning. Adv. Mater. 23(47), 5651–5657.*

occurs which yields a nonlinear pattern on the substrate. This may produce some of the typical shapes such as linear, sinusoidal, side loops, "figure of eight," and circular coiling [118,121], shown in Fig. 2.9c. Therefore, based on the relationship between collector speed and jet speed and the forces imposed on the jet stream, the jet profiles can be categorized into four different shapes, schematically illustrated in Fig. 2.9d. These shapes include the following:

- Case 1: When the collector speed is zero, $S_C = 0$, the jet vertically goes down and starts bending and forming a compressive heel near the collector due to buckling. This deforms the straight jet to a coil shape.

- Case 2: When the collector speed is equal to the jet speed ($S_C = S_j$), the compressive force decreases as the collector speed increases, which reduces the heel region and brings the point of deposition directly under the nozzle.
- Case 3: As the collector speed further increases ($S_C > S_j$), the contact point of the jet and the substrate moves behind that is the point vertically below the nozzle and causes a "lag" region due to a delay in responding to axial tensile force stretching the jet. The delay originates from the viscoelastic properties of the jet.
- Case 4. Upon increasing the collector speed, ($S_C >> S_j$), the lag region is extended, causing further stretching of the jet. However, this phenomenon causes undesirable effects on fibers geometry and location, and consequently affects the quality of final products.

Overall, as suggested by Hutmacher et al. [119], complex patterns and geometries can be produced via matching the translating speed of the collector to the jet speed.

2.4.5 Combining electrospinning with other polymer processing technologies

The combination of polymer processing techniques has also gained a great deal of attention in recent years, as these unique combinations can integrate the advantages of each method and overcome shortcomings observed for using an individual one. For instance, a combination of electrospinning and microfluidic devices could provide a unique opportunity for fabricating fiber meshes of different gradients where the concentrations of various functional agents (e.g., nanoparticles, biomolecules, therapeutic drugs) could be precisely controlled through a microfluidic chip [122]. The combination of AM and electrospinning can also be beneficial for precisely controlling fiber deposition and orientation, as well as pore sizes of scaffolds. Further discussion of such combined approaches have been provided in the following subsections.

2.4.5.1 Electrospinning and microfluidics

One of the major drawbacks of conventional electrospinning is the lack of ability to produce fibers matrices with desired gradients of different materials and physical and chemical signals. Common electrospinning techniques can only produce nanofibers with the same concentration, while matrices with various physicochemical properties are usually required for successfully mimicking tissue engineering constructs or drug delivery applications. To

address this problem and to produce electrospun nanofibers containing gradients of compositions, biomolecules, active chemicals, and nanoparticles, researchers integrated a microfluidic technology with electrospinning [122]. This novel and flexible technique benefits from a Y-shaped microchannel with two inlets and one outlet, where the injection rates of the two different solutions were precisely controlled by a computer (Fig. 2.10). The outlet of the device was connected to a metal tube and subsequently to a thin conductive nozzle. Also, an XYZ-moving platform is used as a substrate to collect nanofibers with different concentrations within the spinning area. This approach enables the creation of matrices with spatially controlled gradients and enhanced functionalities suitable for studying spatial differentiation in mesenchymal stem cells or releasing therapeutic agents in a controlled and preprogrammed fashion.

The use of paper-based microfluidics devices has gained more attention in healthcare, food safety, environmental monitoring, and veterinary medicine [123,124] due to their low cost, simple and rapid fabrication process, compatibility with small volumes of sample, and ease of disposing by incineration with minor environmental consequences [125]. While most of paper-based devices are designed and fabricated in 2D, recently, 3D devices have been fabricated with more functions using paper materials through stacking 2D paper layers or paper origami [126–128]. However, these

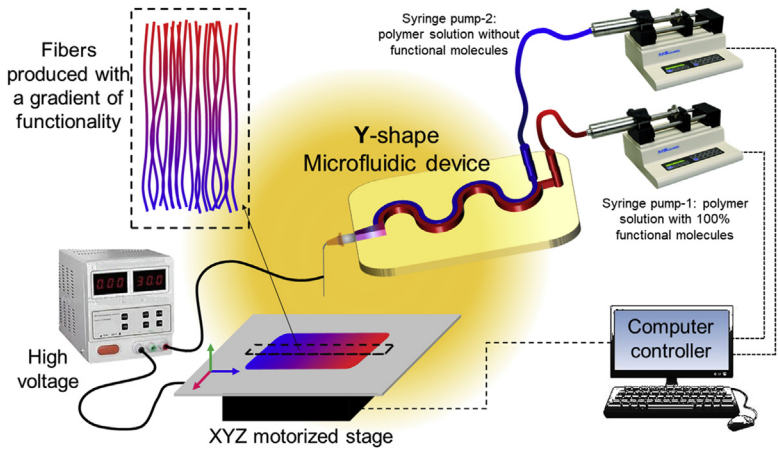

Figure 2.10 Schematic diagram of the platform used to produce nanofibers with different gradient. *Redrawn from Reference Zhang, X., Gao, X., Jiang, L., Qin, J. (2012). Flexible generation of gradient electrospinning nanofibers using a microfluidic assisted approach. Langmuir 28(26), 10026–10032.*

techniques are time consuming and labor-intensive, and the potential misalignment and discontinuity among paper layers and tape layers may affect device performance and confine the reproducibility of the process. Ref. [129] proposed a new technique in which a 3D nanofiber microfluidic device was fabricated using electrospinning and waxing processes controlled by a computer-guided trajectory (Fig. 2.11). The proposed technique could overcome the problems envisaged using old-fashioned methods.

Embedding micro-/nanofibrous structures into microfluidic chips can generate a complex microenvironment for cells for regulating phenotype expression in diagnosis [130], drug screening and discovery research, and tissue engineering applications [131,132]. While an electrospun polymer matrix simulates extracellular matrix for cells, an integrated microfluidic network provides a spatiotemporal liquid microenvironment through velocity and shear force imposed. The potential advantage of such devices was verified by investigating the alignment of neural stem cells in response to the orientation of 2D electrospun matrices versus microfluidic channels. This technique generated a controlled gradient of stromal cell—derived factor 1-alpha [133]. Liu et al. also fabricated a new device via embedding a patterned electrospun fibers into a polydimethylsiloxane (PDMS) microfluidic chip for hepatocyte culture [134]. Under optimized flow conditions, hepatocyte spheroids showed hepatocyte biliary and polarity excretion and

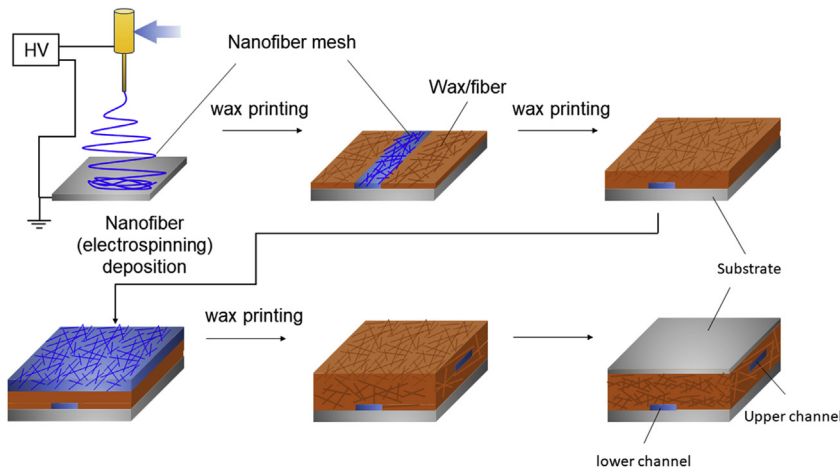

Figure 2.11 Multilayer construct with upper and lower flow channels: fabrication process includes electrospinning nanofibers and printing wax. *Redrawn from Ref. Chen, X., Mo, D., Gong, M. (2020). A flexible method for nanofiber-based 3d microfluidic device fabrication for water quality monitoring. Micromachines 11(3), 276.*

could preserve high levels of urea and albumin secretion for >15 days. The toxic effects of silver nanoparticles (AgNPs) were assessed using this organ-on-a-chip model, where the results indicated consistent and sensitive hepatotoxicity of AgNPs during the experiment.

Although culturing cells on electrospun fibers placed on a solid substrate, as described above, can provide valuable information about the cell attachment, proliferation, expansion, and differentiation, it is often desirable, particularly in biomedical and sensing domains, to utilize a free-standing fibrous micro-/nanostructures. Research findings have proved that a 3D cell culture coupled with online detection and analysis techniques can significantly improve our ability to mimic and understand in vivo systems [135]. Assembled over a channel gap, this novel architecture can provide a more realistic condition for investigating tissue—tissue interface, and for organ tissue engineering, such as liver and lung, where a biomimetic membrane will enable the transport of nutrients as well as wastes while mechanically supporting cells as porous and fibrous structure. However, due to the inherent nature of traditional electrospinning, fabrication of such microdevices still remains a challenge.

Compared to the techniques where fibers are directly generated over a void gap, the postmodifications of electrospun fibers through electromechanical processes [136,137] can be used for creating free-standing fibrous structures. In 2017, Hu et al. [138] introduced a universal, green, and straightforward strategy to produce micropatterned electrospun nanofibers. Their proposed approach utilized a solvent-loaded agarose hydrogel stamp for direct patterning of electrospun nanofibers on a substrate (Fig. 2.12). In general, this method involved the fabrication of an agarose hydrogel stamp by cast molding from a PDMS master. Then, agarose hydrogel stamp was submerged into a solvent—water mixture and subsequently placed over nanofiber meshes (randomly patterned or aligned nanofibers). As the organic solvent in the hydrogel stamp diffused to the nanofiber/stamp interface, it induced a localized coalescence of nanofibers and formed a thin membrane on the contacted zone. Finally, the patterned nanofibers were transferred onto a substrate for further processing. The substrate with patterned electrospun nanofibers was further utilized to spatially coordinate cell orientation in microfluidic devices. Using this technique, complex microstructures can be further fabricated via multistep alteration of microcontact patterning and electrospinning and used for several applications, particularly in biosensing, biomedical engineering, and lab-on-a-chip systems.

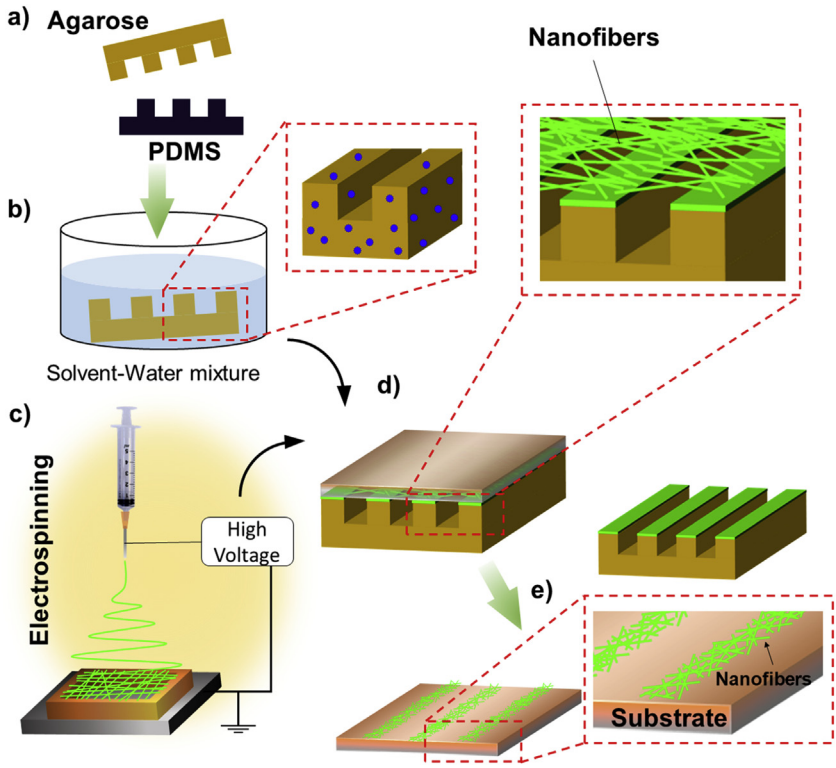

Figure 2.12 Patterning of electrospun nanofibers via solvent-loaded agarose hydrogel stamps. This process involves (a–b) fabrication of solvent-loaded agarose hydrogel, (c) electrospinning nanofibers, (d) contacting electrospun nanofibers with the hydrogel stamp, and (e) transferring nanofibers to a substrate. *Redrawn from Reference Hu, T., Li, Q., Dong, H., Xiao, W., Li, L., Cao, X. (2017). Patterning electrospun nanofibers via agarose hydrogel stamps to spatially coordinate cell orientation in microfluidic device. Small 13(3), 1602610.*

2.4.5.2 Electrospinning and additive manufacturing

A reliable and well-engineered scaffold plays a central role in tissue engineering and regenerative medicine. AM and electrospinning are two separate technologies extensively employed for manufacturing scaffolds in biomedical applications. However, a need to accurately control the pore size and spatial distribution of pores within scaffolds has motivated researchers to combine these two technologies to overcome deficiencies in each method. AM is abroad name for techniques in which an artificial construct is fabricated through layer-by-layer deposition of materials according to a computer-aided design. Although these techniques can precisely control

pores and structure of scaffolds, they usually suffer from low filament resolution not suitable for tissue engineering. In contrast, solution electrospinning can generally produce fibers of different diameters.

As previously mentioned, electrospinning relies on a strong electric field imposed on a viscous fluid, including both polymer solutions and melts, to produce electrified jet passes through the air toward an oppositely charged collector. While electrospinning a polymer solution suffers from different levels of instability originating from inherent properties of the solution and surface charge density, melt electrospinning, which offers lower conductivity and higher viscosity, can produce fibers without such instabilities [139,140]. Further, the charge accumulated with the deposited fibers, especially in solution electrospinning, confines the number of layers which can be deposited and remain bound as one coherent structure. Thus, due to the size of fibers, the thickness of scaffolds produced does not go beyond a few millimeters [116,141]. In addition, typically, solution electrospun meshes have low porosity and form tightly packed structures that only allow cells to proliferate on the mesh surface and restrict cells infiltration into the scaffolds. To overcome some of these challenges, researchers have employed patterned substrates [142,143] or rotating mandrels which allow better prediction and control of the deposition of fibers. However, these processes still lack precisely controlled fiber depositions.

In 2008, researchers reported new fabrication methods via combining AM and electrospinning [144,145]. They fabricated bimodal scaffolds in which the main layers of the structure were formed via FDM, while electrospun fibers were deposited between each of those layers. These scaffolds exhibited large micropores for cells to infiltrate into as well as nanofibrous structures suitable for cell adhesion. Another study showed the advantages of combined electrospinning and FDM to produce tubular architectures for vascular tissue engineering. A more advanced technique has recently been introduced by Huang's group, where they reported the fabrication of intricate suspended fiber architectures. The individual fibers deposited by this technique approach the micrometer/submicrometer scale, while the ultimate height of suspended 3D fiber constructs can span over a centimeter (Fig. 2.13). They also showed an application of the fiber construct in 3D cell culture, where patterned fiber topography was utilized to guide the organization of suspended high-cellular density structures [107]. To further extend the application of 3D fiber constructs for standard biological

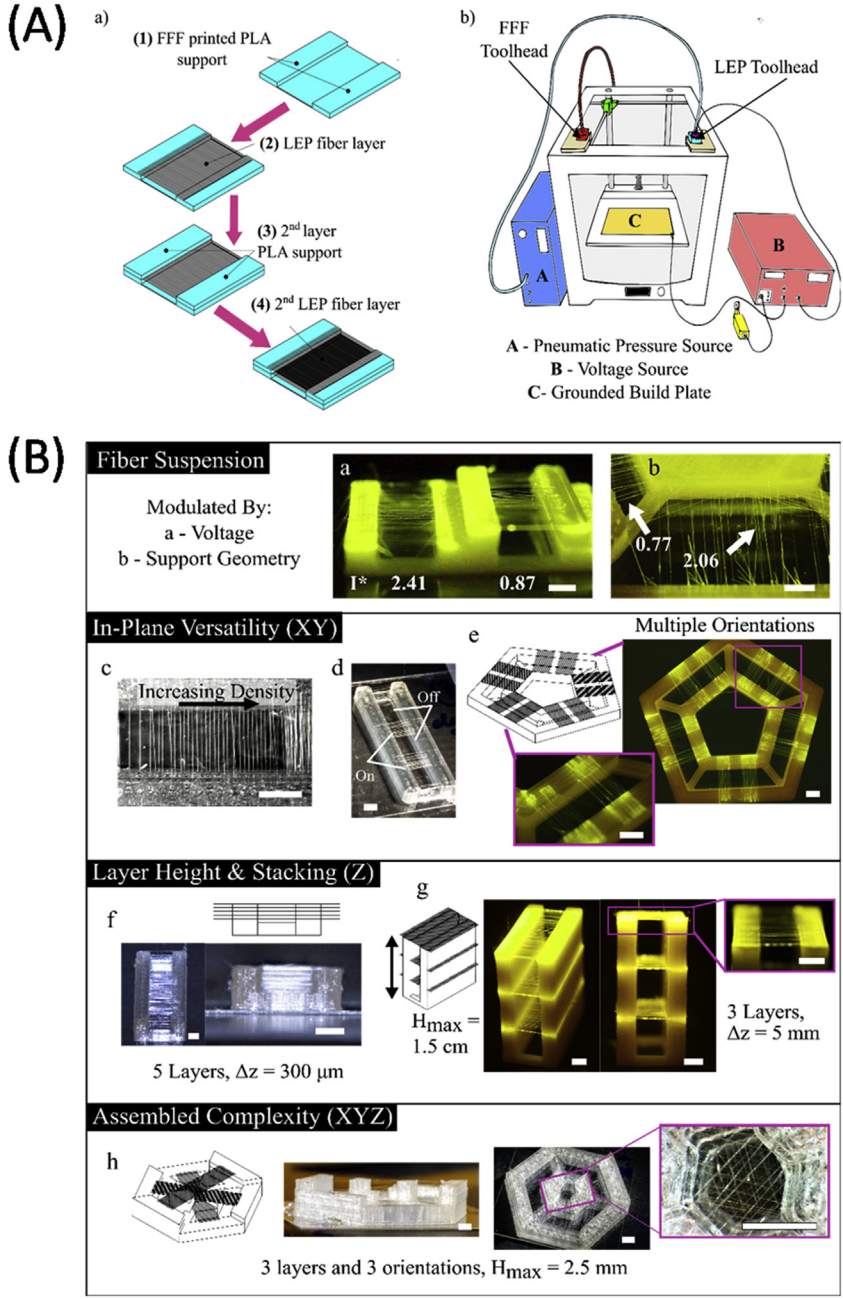

Figure 2.13 (a) Fabrication of bimodal 3D scaffolds via combining near-field electrospinning and additive manufacturing; (b) producing scaffolds of different geometries using the technique introduced in part (a). *Adapted from Reference Gill, E.L., Willis, S., Gerigk, M., Cohen, P., Zhang, D., Li, X., Huang, Y.Y.S. (2019). Fabrication of designable and suspended microfibers via low-voltage 3d micropatterning. ACS Appl. Mater. Interfaces 11(22), 19679—19690 under Creative Commons Attribution 4.0 International license-Open access.*

applications, 3D additive batch electrospinning has been developed to efficiently produce 3D hydrogel gelatin microfiber devices in a batch fashion with minimized sample-to-sample variance [146].

Besides bimodal scaffolds containing microfibrous and nanofibrous features distributed throughout the entire structure, the combination of AM and electrospinning has also been utilized to produce multiphasic constructs containing different regions with different pore size and porosity. Therefore, multiphasic scaffolds could produce adequate artificial tissue microenvironment for different cells to form a functional tissue unit. Hutmacher et al. [147] used this integrated technique to manufacture a multiphasic scaffold and to encapsulate biological agents such as proteins for promoting ectopic periodontal regeneration in rat models. Further details on the combinatorial approaches in electrospinning and 3D printing are covered separately in Chapter 12 of this book by Ameer et al. 2020.

2.5 Summary and future prospects

Electrospinning offers a myriad of design options for functional micro- and nanofiber production for a diverse range of applications. They can be adapted to process a large selection of polymers both of natural and synthetic origin. Other key advantages include that it processes materials in a highly efficient and throughput way. Fibers can be designed in a broad range of sizes [148], mesh porosities [149], and various fiber surface textures. Innovation in the experimental configurations can produce randomly organized fiber networks, highly ordered 2D patterns, and free-standing and stacked fibers. All these can be easily achieved through appropriate material selection, adjusting operating parameters, controlling ambient conditions, and redesigning collectors with particular geometries.

The integration of electrospinning with other manufacturing techniques such as microfluidics has led to enormous progress in tissue engineering and analytical devices for point-of-care diagnosis. It offers versatile advantages for the fabrication of multimaterial constructs with spatial gradients. These innovative and complex architectures could present applications as in vitro models for drug screening, toxicological studies, and cancer research. The combination of electrospinning and AM techniques could also bring a breakthrough for making well-designed constructs via accurately controlling fiber deposition in micro-/nanoscales. This novel combination can fill the need for bimodal and multiphasic scaffolds with systemic variations in morphology. While small-scale architectures are usually produced with

solution electrospinning, these can also be produced via melt electrospinning combined with AM, which together provides higher resolution compared to FDM 3D printers.

Despite the existing achievements with electrospinning, the evolving end-use applications still demand new breakthroughs and improvements of this technique for improving material functionality and device integration. In particular, scaled-up productions for industry purposes and bench-to-bed customization for personalized equipment are of great interest, but yet to be fully addressed. Future developments of electrospinning and fiber production researches could be directed toward integrating with new materials and other advanced material processing and printing approaches.

References

[1] A.K. Yetisen, H. Qu, A. Manbachi, H. Butt, M.R. Dokmeci, J.P. Hinestroza, M. Skorobogatiy, A. Khademhosseini, S.H. Yun, Nanotechnology in textiles, ACS Nano. 10 (3) (2016) 3042–3068.

[2] C.R. Holkar, A.J. Jadhav, D.V. Pinjari, N.M. Mahamuni, A.B. Pandit, A critical review on textile wastewater treatments: possible approaches, J. Environ. Manag. 182 (2016) 351–366.

[3] S. Agarwal, J.H. Wendorff, A. Greiner, Use of electrospinning technique for biomedical applications, Polymer 49 (26) (2008) 5603–5621.

[4] J. Shi, S. Liu, L. Zhang, B. Yang, L. Shu, Y. Yang, M. Ren, Y. Wang, J. Chen, W. Chen, Y. Chai, X. Tao, Smart textile-integrated microelectronic systems for wearable applications, Adv. Mater. 32 (5) (2020) 1901958.

[5] N. Bhardwaj, S.C. Kundu, Electrospinning: a fascinating fiber fabrication technique, Biotechnol. Adv. 28 (3) (2010) 325–347.

[6] J. Xue, T. Wu, Y. Dai, Y. Xia, Electrospinning and electrospun nanofibers: methods, materials, and applications, Chem. Rev. 119 (8) (2019) 5298–5415.

[7] C.V. Boys, On the production, properties, and some suggested uses of the finest threads, Proc. Phys. Soc. Lond. 9 (1) (1887) 8–19.

[8] J. Doshi, D.H. Reneker, Electrospinning process and applications of electrospun fibers, J. Electrost. 35 (2) (1995) 151–160.

[9] D. Li, Y. Xia, Electrospinning of nanofibers: reinventing the wheel? Adv. Mater. 16 (14) (2004) 1151–1170.

[10] C. Chang, V.H. Tran, J. Wang, Y.-K. Fuh, L. Lin, Direct-write piezoelectric polymeric nanogenerator with high energy conversion efficiency, Nano. Lett. 10 (2) (2010) 726–731.

[11] W. Wang, P.N. Stipp, K. Ouaras, S. Fathi, Y.Y.S. Huang, Broad bandwidth, self-powered acoustic sensor created by dynamic near-field electrospinning of suspended, transparent piezoelectric nanofiber mesh, Small 16 (28) (2020) 2000581.

[12] Y. Huang, X. Bai, M. Zhou, S. Liao, Z. Yu, Y. Wang, H. Wu, Large-scale spinning of silver nanofibers as flexible and reliable conductors, Nano. Lett. 16 (9) (2016) 5846–5851.

[13] W. Wenyu, O. Karim, L.,R. Alexandra, L. Xia, G. Magda, N. Tobias, M. George, H. Yan Yan Shery, Inflight fluidic fibre printing towards array and 3d optoelectronic and sensing architectures, Sci. Adv. 6 (40) (2020) eaba0931.
[14] T.D. Brown, P.D. Dalton, D.W. Hutmacher, Melt electrospinning today: an opportune time for an emerging polymer process, Prog. Polym. Sci. 56 (2016) 116–166.
[15] R.T. Collins, J.J. Jones, M.T. Harris, O.A. Basaran, Electrohydrodynamic tip streaming and emission of charged drops from liquid cones, Nat. Phys. 4 (2) (2008) 149–154.
[16] D.H. Reneker, A.L. Yarin, Electrospinning jets and polymer nanofibers, Polymer 49 (10) (2008) 2387–2425.
[17] T. Subbiah, G.S. Bhat, R.W. Tock, S. Parameswaran, S.S. Ramkumar, Electrospinning of nanofibers, J. Appl. Polym. Sci. 96 (2) (2005) 557–569.
[18] C.J. Luo, S.D. Stoyanov, E. Stride, E. Pelan, M. Edirisinghe, Electrospinning versus fibre production methods: from specifics to technological convergence, Chem. Soc. Rev. 41 (13) (2012) 4708–4735.
[19] D.H. Reneker, A.L. Yarin, H. Fong, S. Koombhongse, Bending instability of electrically charged liquid jets of polymer solutions in electrospinning, J. Appl. Phys. 87 (9) (2000) 4531–4547.
[20] Z.-M. Huang, Y.Z. Zhang, M. Kotaki, S. Ramakrishna, A review on polymer nanofibers by electrospinning and their applications in nanocomposites, Compos. Sci. Technol. 63 (15) (2003) 2223–2253.
[21] S. Koombhongse, W. Liu, D.H. Reneker, Flat polymer ribbons and other shapes by electrospinning, J. Polym. Sci. B Polym. Phys. 39 (21) (2001) 2598–2606.
[22] G. Yang, X. Li, Y. He, J. Ma, G. Ni, S. Zhou, From nano to micro to macro: electrospun hierarchically structured polymeric fibers for biomedical applications, Prog. Polym. Sci. 81 (2018) 80–113.
[23] S. Chen, R. Li, X. Li, J. Xie, Electrospinning: an enabling nanotechnology platform for drug delivery and regenerative medicine, Adv. Drug Deliv. Rev. 132 (2018b) 188–213.
[24] C. Drew, X. Wang, L.A. Samuelson, J. Kumar, The effect of viscosity and filler on electrospun fiber morphology, J. Macromol. Sci., Part A 40 (12) (2003) 1415–1422.
[25] H. Fong, I. Chun, D.H. Reneker, Beaded nanofibers formed during electrospinning, Polymer 40 (16) (1999) 4585–4592.
[26] T. Jarusuwannapoom, W. Hongrojjanawiwat, S. Jitjaicham, L. Wannatong, M. Nithitanakul, C. Pattamaprom, P. Koombhongse, R. Rangkupan, P. Supaphol, Effect of solvents on electro-spinnability of polystyrene solutions and morphological appearance of resulting electrospun polystyrene fibers, Eur. Polym. J. 41 (3) (2005) 409–421.
[27] C.S. Ki, D.H. Baek, K.D. Gang, K.H. Lee, I.C. Um, Y.H. Park, Characterization of gelatin nanofiber prepared from gelatin–formic acid solution, Polymer 46 (14) (2005) 5094–5102.
[28] P. Gupta, C. Elkins, T.E. Long, G.L. Wilkes, Electrospinning of linear homopolymers of poly(methyl methacrylate): exploring relationships between fiber formation, viscosity, molecular weight and concentration in a good solvent, Polymer 46 (13) (2005) 4799–4810.
[29] C.L. Casper, J.S. Stephens, N.G. Tassi, D.B. Chase, J.F. Rabolt, Controlling surface morphology of electrospun polystyrene fibers: Effect of humidity and molecular weight in the electrospinning process, Macromolecules 37 (2) (2004) 573–578.
[30] G.C. Rutledge, S.V. Fridrikh, Formation of fibers by electrospinning, Adv. Drug Deliv. Rev. 59 (14) (2007) 1384–1391.

[31] H. Nie, A. He, J. Zheng, S. Xu, J. Li, C.C. Han, Effects of chain conformation and entanglement on the electrospinning of pure alginate, Biomacromolecules 9 (5) (2008) 1362–1365.
[32] S.L. Shenoy, W.D. Bates, H.L. Frisch, G.E. Wnek, Role of chain entanglements on fiber formation during electrospinning of polymer solutions: good solvent, non-specific polymer–polymer interaction limit, Polymer 46 (10) (2005) 3372–3384.
[33] J. Lin, B. Ding, J. Yu, Y. Hsieh, Direct fabrication of highly nanoporous polystyrene fibers via electrospinning, ACS Appl. Mater. Interface. 2 (2) (2010) 521–528.
[34] A. Omidinia-Anarkoli, R. Rimal, Y. Chandorkar, D.B. Gehlen, J.C. Rose, K. Rahimi, T. Haraszti, L. De Laporte, Solvent-induced nanotopographies of single microfibers regulate cell mechanotransduction, ACS Appl. Mater. Interface. 11 (8) (2019) 7671–7685.
[35] F.-L. Zhou, P.L. Hubbard, S.J. Eichhorn, G.J.M. Parker, Jet deposition in near-field electrospinning of patterned polycaprolactone and sugar-polycaprolactone core–shell fibres, Polymer 52 (16) (2011) 3603–3610.
[36] T. Yao, H. Chen, P. Samal, S. Giselbrecht, M.B. Baker, L. Moroni, Self-assembly of electrospun nanofibers into gradient honeycomb structures, Mater. Des. 168 (2019) 107614.
[37] X. Zong, K. Kim, D. Fang, S. Ran, B.S. Hsiao, B. Chu, Structure and process relationship of electrospun bioabsorbable nanofiber membranes, Polymer 43 (16) (2002) 4403–4412.
[38] R. Middleton, X. Li, J. Shepherd, Z. Li, W. Wang, S.M. Best, R.E. Cameron, Y.Y.S. Huang, Near-field electrospinning patterning polycaprolactone and polycaprolactone/collagen interconnected fiber membrane, Macromol. Mater. Eng. 303 (2) (2018) 1700463.
[39] M. Bognitzki, W. Czado, T. Frese, A. Schaper, M. Hellwig, M. Steinhart, A. Greiner, J.H. Wendorff, Nanostructured fibers via electrospinning, Adv. Mater. 13 (1) (2001) 70–72.
[40] Y. Hong, X. Chen, X. Jing, H. Fan, B. Guo, Z. Gu, X. Zhang, Preparation, bioactivity, and drug release of hierarchical nanoporous bioactive glass ultrathin fibers, Adv. Mater. 22 (6) (2010) 754–758.
[41] N. Amariei, L.R. Manea, A.P. Bertea, A. Bertea, A. Popa, The influence of polymer solution on the properties of electrospun 3d nanostructures, IOP Conf. Ser. Mater. Sci. Eng. 209 (2017) 012092.
[42] I.S. Chronakis, S. Grapenson, A. Jakob, Conductive polypyrrole nanofibers via electrospinning: electrical and morphological properties, Polymer 47 (5) (2006) 1597–1603.
[43] C. Mit-uppatham, M. Nithitanakul, P. Supaphol, Ultrafine electrospun polyamide-6 fibers: effect of solution conditions on morphology and average fiber diameter, Macromol. Chem. Phys. 205 (17) (2004) 2327–2338.
[44] M.M. Demir, I. Yilgor, E. Yilgor, B. Erman, Electrospinning of polyurethane fibers, Polymer 43 (11) (2002) 3303–3309.
[45] C. Huang, S. Chen, C. Lai, D.H. Reneker, H. Qiu, Y. Ye, H. Hou, Electrospun polymer nanofibres with small diameters, Nanotechnology 17 (6) (2006) 1558–1563.
[46] H. Chen, X. Huang, M. Zhang, F. Damanik, M.B. Baker, A. Leferink, H. Yuan, R. Truckenmüller, C. van Blitterswijk, L. Moroni, Tailoring surface nanoroughness of electrospun scaffolds for skeletal tissue engineering, Acta Biomater. 59 (2017a) 82–93.
[47] S. De Vrieze, T. Van Camp, A. Nelvig, B. Hagström, P. Westbroek, K. De Clerck, The effect of temperature and humidity on electrospinning, J. Mater. Sci. 44 (5) (2009) 1357–1362.

[48] J. Pelipenko, J. Kristl, B. Janković, S. Baumgartner, P. Kocbek, The impact of relative humidity during electrospinning on the morphology and mechanical properties of nanofibers, Int. J. Pharm. 456 (1) (2013) 125−134.
[49] C. Wang, H.-S. Chien, C.-H. Hsu, Y.-C. Wang, C.-T. Wang, H.-A. Lu, Electrospinning of polyacrylonitrile solutions at elevated temperatures, Macromolecules 40 (22) (2007) 7973−7983.
[50] P. Lu, Y. Xia, Maneuvering the internal porosity and surface morphology of electrospun polystyrene yarns by controlling the solvent and relative humidity, Langmuir 29 (23) (2013) 7070−7078.
[51] W. Zuo, M. Zhu, W. Yang, H. Yu, Y. Chen, Y. Zhang, Experimental study on relationship between jet instability and formation of beaded fibers during electrospinning, Polym. Eng. Sci. 45 (5) (2005) 704−709.
[52] C.J. Thompson, G.G. Chase, A.L. Yarin, D.H. Reneker, Effects of parameters on nanofiber diameter determined from electrospinning model, Polymer 48 (23) (2007) 6913−6922.
[53] C. Zhang, X. Yuan, L. Wu, Y. Han, J. Sheng, Study on morphology of electrospun poly(vinyl alcohol) mats, Eur. Polym. J. 41 (3) (2005) 423−432.
[54] J. Doshi, D.H. Reneker, Electrospinning Process and Applications of Electrospun Fibers, Conference Record of the 1993 IEEE Industry Applications Conference Twenty-Eighth IAS Annual Meeting, vol. 1693, 1993, pp. 1698−1703.
[55] S. Chen, S.K. Boda, S.K. Batra, X. Li, J. Xie, Emerging roles of electrospun nanofibers in cancer research, Advanced Healthcare Materials 7 (6) (2018a) 1701024.
[56] K. Ghaseminezhad, M. Zare, S. Lashkarara, M. Yousefzadeh, J. Aghazadeh Mohandesi, Fabrication of althea officinalis loaded electrospun nanofibrous scaffold for potential application of skin tissue engineering, J. Appl. Polym. Sci. 137 (16) (2020) 48587.
[57] Z. Tashi, M. Zare, N. Parvin, Application of phytic-acid as an in-situ crosslinking agent in electrospun gelatin-based scaffolds for skin tissue engineering, Mater. Lett. 264 (2020) 127275.
[58] I.G. Loscertales, A. Barrero, I. Guerrero, R. Cortijo, M. Marquez, A.M. Gañán-Calvo, Micro/nano encapsulation via electrified coaxial liquid jets, Science 295 (5560) (2002) 1695−1698.
[59] L. Xiaoyan, H. Tao, W. Yitao, C. Xiao, H. Yiyong, Y. Dengguang, Innovation Training-From Analogy to Deepen Comprehension and to Innovation with Modified Coaxial Electrospinning as an Example, 2018 2nd International Conference on Management, Education and Social Science (ICMESS 2018), Atlantis Press, 2018.
[60] D. Han, A.J. Steckl, Triaxial electrospun nanofiber membranes for controlled dual release of functional molecules, ACS Appl. Mater. Interfaces 5 (16) (2013) 8241−8245.
[61] A. Khalf, K. Singarapu, S.V. Madihally, Influence of solvent characteristics in triaxial electrospun fiber formation, React. Funct. Polym. 90 (2015) 36−46.
[62] J. Jiang, G. Zheng, X. Wang, W. Li, G. Kang, H. Chen, S. Guo, J. Liu, Arced multinozzle electrospinning spinneret for high-throughput production of nanofibers, Micromachines 11 (1) (2020) 27.
[63] G. Zheng, J. Jiang, D. Chen, J. Liu, Y. Liu, J. Zheng, X. Wang, W. Li, Multinozzle high efficiency electrospinning with the constraint of sheath gas, J. Appl. Polym. Sci. 136 (22) (2019) 47574.
[64] N. Wang, H. Chen, L. Lin, Y. Zhao, X. Cao, Y. Song, L. Jiang, Multicomponent phase change microfibers prepared by temperature control multifluidic electrospinning, Macromol. Rapid Commun. 31 (18) (2010) 1622−1627.

[65] X. Tian, H. Bai, Y. Zheng, L. Jiang, Bio-inspired heterostructured bead-on-string fibers that respond to environmental wetting, Adv. Funct. Mater. 21 (8) (2011) 1398–1402.
[66] Y. Jin, D. Yang, D. Kang, X. Jiang, Fabrication of necklace-like structures via electrospinning, Langmuir 26 (2) (2010) 1186–1190.
[67] W. Yuan, K.-Q. Zhang, Structural evolution of electrospun composite fibers from the blend of polyvinyl alcohol and polymer nanoparticles, Langmuir 28 (43) (2012) 15418–15424.
[68] Y. Sun, R.B. Sills, X. Hu, Z.W. Seh, X. Xiao, H. Xu, W. Luo, H. Jin, Y. Xin, T. Li, Z. Zhang, J. Zhou, W. Cai, Y. Huang, Y. Cui, A bamboo-inspired nanostructure design for flexible, foldable, and twistable energy storage devices, Nano. Lett. 15 (6) (2015) 3899–3906.
[69] H. Niu, T. Lin, X. Wang, Needleless electrospinning. I. A comparison of cylinder and disk nozzles, J. Appl. Polym. Sci. 114 (6) (2009) 3524–3530.
[70] R. Yang, J. He, L. Xu, J. Yu, Bubble-electrospinning for fabricating nanofibers, Polymer 50 (24) (2009) 5846–5850.
[71] A. Becker, H. Zernetsch, M. Mueller, B. Glasmacher, A novel coaxial nozzle for in-process adjustment of electrospun scaffolds' fiber diameter, Curr. Direct. Biomed. Eng. 1 (1) (2015) 104–107.
[72] E. Smit, U. Bűttner, R.D. Sanderson, Continuous yarns from electrospun fibers, Polymer 46 (8) (2005) 2419–2423.
[73] W.-E. Teo, R. Gopal, R. Ramaseshan, K. Fujihara, S. Ramakrishna, A dynamic liquid support system for continuous electrospun yarn fabrication, Polymer 48 (12) (2007) 3400–3405.
[74] R. Solberg, Position-controlled Deposition for Electrospinning, Department Mechanical Engineering, 2007.
[75] D. Li, Y. Wang, Y. Xia, Electrospinning nanofibers as uniaxially aligned arrays and layer-by-layer stacked films, Adv. Mater. 16 (4) (2004) 361–366.
[76] P.D. Dalton, D. Klee, M. Möller, Electrospinning with dual collection rings, Polymer 46 (3) (2005) 611–614.
[77] T.D. Brown, F. Edin, N. Detta, A.D. Skelton, D.W. Hutmacher, P.D. Dalton, Melt electrospinning of poly(ε-caprolactone) scaffolds: phenomenological observations associated with collection and direct writing, Mater. Sci. Eng. C 45 (2014) 698–708.
[78] B. Sundaray, V. Subramanian, T.S. Natarajan, R.-Z. Xiang, C.-C. Chang, W.-S. Fann, Electrospinning of continuous aligned polymer fibers, Appl. Phys. Lett. 84 (7) (2004) 1222–1224.
[79] W.E. Teo, M. Kotaki, X.M. Mo, S. Ramakrishna, Porous tubular structures with controlled fibre orientation using a modified electrospinning method, Nanotechnology 16 (6) (2005) 918–924.
[80] A. Theron, E. Zussman, A.L. Yarin, Electrostatic field-assisted alignment of electrospun nanofibres, Nanotechnology 12 (3) (2001) 384–390.
[81] S.A. Harfenist, S.D. Cambron, E.W. Nelson, S.M. Berry, A.W. Isham, M.M. Crain, K.M. Walsh, R.S. Keynton, R.W. Cohn, Direct drawing of suspended filamentary micro- and nanostructures from liquid polymers, Nano. Lett. 4 (10) (2004) 1931–1937.
[82] Y. Liu, G. Ma, D. Fang, J. Xu, H. Zhang, J. Nie, Effects of solution properties and electric field on the electrospinning of hyaluronic acid, Carbohydr. Polym. 83 (2) (2011) 1011–1015.
[83] D. Li, Y. Wang, Y. Xia, Electrospinning of polymeric and ceramic nanofibers as uniaxially aligned arrays, Nano. Lett. 3 (8) (2003) 1167–1171.

[84] X. Chen, L. Cheng, H. Li, A. Barhoum, Y. Zhang, X. He, W. Yang, M.M. Bubakir, H. Chen, Magnetic nanofibers: unique properties, fabrication techniques, and emerging applications, Chemistry 3 (31) (2018c) 9127–9143.
[85] Y. Liu, X. Zhang, Y. Xia, H. Yang, Magnetic-field-assisted electrospinning of aligned straight and wavy polymeric nanofibers, Adv. Mater. 22 (22) (2010) 2454–2457.
[86] D. Yang, B. Lu, Y. Zhao, X. Jiang, Fabrication of aligned fibrous arrays by magnetic electrospinning, Adv. Mater. 19 (21) (2007) 3702–3706.
[87] S.M. Park, S. Eom, W. Kim, D.S. Kim, Role of grounded liquid collectors in precise patterning of electrospun nanofiber mats, Langmuir 34 (1) (2018) 284–290.
[88] Y. Xin, D.H. Reneker, Hierarchical polystyrene patterns produced by electrospinning, Polymer 53 (19) (2012) 4254–4261.
[89] D. Duft, T. Achtzehn, R. Müller, B.A. Huber, T. Leisner, Rayleigh jets from levitated microdroplets, Nature 421 (6919) (2003), 128-128.
[90] D.H. Reneker, H. Fong, Polymeric Nanofibers, ACS Publications, 2006.
[91] L.K. Lim, J. Hua, C.-H. Wang, K.A. Smith, Numerical simulation of cone-jet formation in electrohydrodynamic atomization, AIChE J. 57 (1) (2011) 57–78.
[92] J. Xie, J. Jiang, P. Davoodi, M.P. Srinivasan, C.-H. Wang, Electrohydrodynamic atomization: a two-decade effort to produce and process micro-/nanoparticulate materials, Chem. Eng. Sci. 125 (2015) 32–57.
[93] W.-C. Yan, P. Davoodi, Y.W. Tong, C.-H. Wang, Computational study of core-shell droplet formation in coaxial electrohydrodynamic atomization process, AICHE J. 62 (12) (2016) 4259–4276.
[94] M.E. Helgeson, K.N. Grammatikos, J.M. Deitzel, N.J. Wagner, Theory and kinematic measurements of the mechanics of stable electrospun polymer jets, Polymer 49 (12) (2008) 2924–2936.
[95] D.H. Reneker, W. Kataphinan, A. Theron, E. Zussman, A.L. Yarin, Nanofiber garlands of polycaprolactone by electrospinning, Polymer 43 (25) (2002) 6785–6794.
[96] A.M. Gañán-Calvo, Cone-jet analytical extension of taylor's electrostatic solution and the asymptotic universal scaling laws in electrospraying, Phys. Rev. Lett. 79 (2) (1997) 217–220.
[97] J.-H. He, Y. Wu, W.-W. Zuo, Critical length of straight jet in electrospinning, Polymer 46 (26) (2005) 12637–12640.
[98] D. Sun, C. Chang, S. Li, L. Lin, Near-field electrospinning, Nano. Lett. 6 (4) (2006) 839–842.
[99] G.S. Bisht, G. Canton, A. Mirsepassi, L. Kulinsky, S. Oh, D. Dunn-Rankin, M.J. Madou, Controlled continuous patterning of polymeric nanofibers on three-dimensional substrates using low-voltage near-field electrospinning, Nano. Lett. 11 (4) (2011) 1831–1837.
[100] H. Chen, A.d.B.F.B. Malheiro, C. van Blitterswijk, C. Mota, P.A. Wieringa, L. Moroni, Direct writing electrospinning of scaffolds with multidimensional fiber architecture for hierarchical tissue engineering, ACS Appl. Mater. Interfaces 9 (44) (2017b) 38187–38200.
[101] Y. Huang, Y. Duan, Y. Ding, N. Bu, Y. Pan, N. Lu, Z. Yin, Versatile, kinetically controlled, high precision electrohydrodynamic writing of micro/nanofibers, Sci. Rep. 4 (1) (2014) 5949.
[102] N. Xue, X. Li, C. Bertulli, Z. Li, A. Patharagulpong, A. Sadok, Y.Y.S. Huang, Rapid patterning of 1-d collagenous topography as an ecm protein fibril platform for image cytometry, PloS One 9 (4) (2014) e93590.
[103] Y.M. Shin, M.M. Hohman, M.P. Brenner, G.C. Rutledge, Experimental characterization of electrospinning: the electrically forced jet and instabilities, Polymer 42 (25) (2001) 09955–09967.

[104] G. Zheng, W. Li, X. Wang, D. Wu, D. Sun, L. Lin, Precision deposition of a nanofibre by near-field electrospinning, J. Phys. Appl. Phys. 43 (41) (2010) 415501.
[105] L. Kong, G.R. Ziegler, Rheological aspects in fabricating pullulan fibers by electro-wet-spinning, Food Hydrocolloids 38 (2014) 220−226.
[106] R. Chang, J. Nam, W. Sun, Effects of dispensing pressure and nozzle diameter on cell survival from solid freeform fabrication−based direct cell writing, Tissue Eng. 14 (1) (2008) 41−48.
[107] E.L. Gill, S. Willis, M. Gerigk, P. Cohen, D. Zhang, X. Li, Y.Y.S. Huang, Fabrication of designable and suspended microfibers via low-voltage 3d micropatterning, ACS Appl. Mater. Interface. 11 (22) (2019) 19679−19690.
[108] X. Li, Z. Li, L. Wang, G. Ma, F. Meng, R.H. Pritchard, E.L. Gill, Y. Liu, Y.Y.S. Huang, Low-voltage continuous electrospinning patterning, ACS Appl. Mater. Interface. 8 (47) (2016) 32120−32131.
[109] Z. Li, I.M. Lei, P. Davoodi, L. Huleihel, Y.Y.S. Huang, Solution formulation and rheology for fabricating extracellular matrix-derived fibers using low-voltage electrospinning patterning, ACS Biomater. Sci. Eng. 5 (7) (2019) 3676−3684.
[110] Z. Li, J. Tuffin, I.M. Lei, F.S. Ruggeri, N.S. Lewis, E.L. Gill, T. Savin, L. Huleihel, S.F. Badylak, T. Knowles, S.C. Satchell, G.I. Welsh, M.A. Saleem, Y.Y.S. Huang, Solution fibre spinning technique for the fabrication of tuneable decellularised matrix-laden fibres and fibrous micromembranes, Acta Biomater. 78 (2018) 111−122.
[111] J.A. Lewis, Direct ink writing of 3d functional materials, Adv. Funct. Mater. 16 (17) (2006) 2193−2204.
[112] C. Hellmann, J. Belardi, R. Dersch, A. Greiner, J.H. Wendorff, S. Bahnmueller, High precision deposition electrospinning of nanofibers and nanofiber nonwovens, Polymer 50 (5) (2009) 1197−1205.
[113] S.H. Ahn, H.J. Lee, G.H. Kim, Polycaprolactone scaffolds fabricated with an advanced electrohydrodynamic direct-printing method for bone tissue regeneration, Biomacromolecules 12 (12) (2011) 4256−4263.
[114] J. Lee, S.Y. Lee, J. Jang, Y.H. Jeong, D.-W. Cho, Fabrication of patterned nanofibrous mats using direct-write electrospinning, Langmuir 28 (18) (2012) 7267−7275.
[115] E. Zhmayev, D. Cho, Y. Lak Joo, Electrohydrodynamic quenching in polymer melt electrospinning, Phys. Fluid. 23 (7) (2011) 073102.
[116] P.D. Dalton, C. Vaquette, B.L. Farrugia, T.R. Dargaville, T.D. Brown, D.W. Hutmacher, Electrospinning and additive manufacturing: converging technologies, Biomaterial. Sci. 1 (2) (2013) 171−185.
[117] C.B. Dayan, F. Afghah, B.S. Okan, M. Yıldız, Y. Menceloglu, M. Culha, B. Koc, Modeling 3d melt electrospinning writing by response surface methodology, Mater. Des. 148 (2018) 87−95.
[118] H. Gernot, Y. Almoatazbellah, H. Andrei, N.H. Jodie, J. Tomasz, G. Jürgen, D.D. Paul, Fibre pulsing during melt electrospinning writing, BioNanoMaterials 17 (3−4) (2016) 159−171.
[119] T.D. Brown, P.D. Dalton, D.W. Hutmacher, Direct writing by way of melt electrospinning, Adv. Mater. 23 (47) (2011) 5651−5657.
[120] F.M. Au - Wunner, O. Au - Bas, N.T. Au - Saidy, P.D. Au - Dalton, E.M.D.-J. Au - Pardo, D.W. Au - Hutmacher, Melt electrospinning writing of three-dimensional poly(ε-caprolactone) scaffolds with controllable morphologies for tissue engineering applications, JoVE 130 (2017) e56289.
[121] T. Jungst, M.L. Muerza-Cascante, T.D. Brown, M. Standfest, D.W. Hutmacher, J. Groll, P.D. Dalton, Melt electrospinning onto cylinders: effects of rotational velocity and collector diameter on morphology of tubular structures, Polym. Int. 64 (9) (2015) 1086−1095.

[122] X. Zhang, X. Gao, L. Jiang, J. Qin, Flexible generation of gradient electrospinning nanofibers using a microfluidic assisted approach, Langmuir 28 (26) (2012) 10026−10032.
[123] H.N. Chan, Y. Shu, B. Xiong, Y. Chen, Y. Chen, Q. Tian, S.A. Michael, B. Shen, H. Wu, Simple, cost-effective 3d printed microfluidic components for disposable, point-of-care colorimetric analysis, ACS Sens. 1 (3) (2016) 227−234.
[124] A.K. Yetisen, M.S. Akram, C.R. Lowe, Paper-based microfluidic point-of-care diagnostic devices, Lab Chip 13 (12) (2013) 2210−2251.
[125] Y. Zhang, L. Zhang, K. Cui, S. Ge, X. Cheng, M. Yan, J. Yu, H. Liu, Flexible electronics based on micro/nanostructured paper, Adv. Mater. 30 (51) (2018) 1801588.
[126] L. Ge, S. Wang, X. Song, S. Ge, J. Yu, 3d origami-based multifunction-integrated immunodevice: low-cost and multiplexed sandwich chemiluminescence immunoassay on microfluidic paper-based analytical device, Lab Chip 12 (17) (2012) 3150−3158.
[127] A.W. Martinez, S.T. Phillips, G.M. Whitesides, Three-dimensional microfluidic devices fabricated in layered paper and tape, Proc. Natl. Acad. Sci. U. S. A. 105 (50) (2008) 19606−19611.
[128] J. Reboud, G. Xu, A. Garrett, M. Adriko, Z. Yang, E.M. Tukahebwa, C. Rowell, J.M. Cooper, Paper-based microfluidics for DNA diagnostics of malaria in low resource underserved rural communities, Proc. Natl. Acad. Sci. U. S. A. 116 (11) (2019) 4834−4842.
[129] X. Chen, D. Mo, M. Gong, A flexible method for nanofiber-based 3d microfluidic device fabrication for water quality monitoring, Micromachines 11 (3) (2020) 276.
[130] Z. Rezaei, M. Mahmoudifard, Pivotal role of electrospun nanofibers in microfluidic diagnostic systems − a review, J. Mater. Chem. B 7 (30) (2019) 4602−4619.
[131] Z. He, N. Ranganathan, P. Li, Evaluating nanomedicine with microfluidics, Nanotechnology 29 (49) (2018) 492001.
[132] Y. Liu, K. Hu, Y. Wang, Primary hepatocytes cultured on a fiber-embedded pdms chip to study drug metabolism, Polymers 9 (6) (2017) 215.
[133] P. Wallin, C. Zandén, B. Carlberg, N. Hellström Erkenstam, J. Liu, J. Gold, A method to integrate patterned electrospun fibers with microfluidic systems to generate complex microenvironments for cell culture applications, Biomicrofluidics 6 (2) (2012) 024131.
[134] Y. Liu, S. Wang, Y. Wang, Patterned fibers embedded microfluidic chips based on pla and pdms for ag nanoparticle safety testing, Polymers 8 (11) (2016) 402.
[135] A.D. Castiaux, D.M. Spence, R.S. Martin, Review of 3d cell culture with analysis in microfluidic systems, Analyt. Method. 11 (33) (2019) 4220−4232.
[136] B. Carlberg, T. Wang, J. Liu, Direct photolithographic patterning of electrospun films for defined nanofibrillar microarchitectures, Langmuir 26 (4) (2010) 2235−2239.
[137] Y. Liu, L. Zhang, H. Li, S. Yan, J. Yu, J. Weng, X. Li, Electrospun fibrous mats on lithographically micropatterned collectors to control cellular behaviors, Langmuir 28 (49) (2012) 17134−17142.
[138] T. Hu, Q. Li, H. Dong, W. Xiao, L. Li, X. Cao, Patterning electrospun nanofibers via agarose hydrogel stamps to spatially coordinate cell orientation in microfluidic device, Small 13 (3) (2017) 1602610.
[139] P.D. Dalton, D. Grafahrend, K. Klinkhammer, D. Klee, M. Möller, Electrospinning of polymer melts: phenomenological observations, Polymer 48 (23) (2007) 6823−6833.
[140] H. Zhou, T.B. Green, Y.L. Joo, The thermal effects on electrospinning of polylactic acid melts, Polymer 47 (21) (2006) 7497−7505.
[141] C. Vaquette, J. Cooper-White, The use of an electrostatic lens to enhance the efficiency of the electrospinning process, Cell Tissue Res. 347 (3) (2012) 815−826.

[142] C. Vaquette, J.J. Cooper-White, Increasing electrospun scaffold pore size with tailored collectors for improved cell penetration, Acta Biomater. 7 (6) (2011) 2544–2557.
[143] D. Zhang, J. Chang, Patterning of electrospun fibers using electroconductive templates, Adv. Mater. 19 (21) (2007) 3664–3667.
[144] G. Kim, J. Son, S. Park, W. Kim, Hybrid process for fabricating 3d hierarchical scaffolds combining rapid prototyping and electrospinning, Macromol. Rapid Commun. 29 (19) (2008) 1577–1581.
[145] S.H. Park, T.G. Kim, H.C. Kim, D.-Y. Yang, T.G. Park, Development of dual scale scaffolds via direct polymer melt deposition and electrospinning for applications in tissue regeneration, Acta Biomater. 4 (5) (2008) 1198–1207.
[146] E.L. Gill, W. Wang, R. Liu, Y.Y.S. Huang, Additive batch electrospinning patterning of tethered gelatin hydrogel fibres with swelling-induced fibre curling, Addit. Manufact. 36 (2020) 101456.
[147] C. Vaquette, W. Fan, Y. Xiao, S. Hamlet, D.W. Hutmacher, S. Ivanovski, A biphasic scaffold design combined with cell sheet technology for simultaneous regeneration of alveolar bone/periodontal ligament complex, Biomaterial. 33 (22) (2012) 5560–5573.
[148] Z. Wang, Y. Cui, J. Wang, X. Yang, Y. Wu, K. Wang, X. Gao, D. Li, Y. Li, X.-L. Zheng, Y. Zhu, D. Kong, Q. Zhao, The effect of thick fibers and large pores of electrospun poly(ε-caprolactone) vascular grafts on macrophage polarization and arterial regeneration, Biomaterials 35 (22) (2014) 5700–5710.
[149] A. Hrynevich, B.Ş. Elçi, J.N. Haigh, R. McMaster, A. Youssef, C. Blum, T. Blunk, G. Hochleitner, J. Groll, P.D. Dalton, Dimension-based design of melt electrowritten scaffolds, Small 14 (22) (2018) 1800232.